ADVANCED MATERIALS

DOI: 10.1002/adma.200701254

Direct Delivery and Submicrometer Patterning of DNA by a Nanofountain Probe**

By *Keun-Ho Kim*, *Raymond G. Sanedrin*, *Andrea M. Ho*, *Seung W. Lee*, *Nicolaie Moldovan*, *Chad A. Mirkin*, and *Horacio D. Espinosa**

Nanopatterning of biological materials has significant potential in life sciences and medicine because highly miniaturized structures provide routes to high-density combinatorial libraries and ways of manipulating biological structures (proteins, viruses, and cells) at the single particle level.[1–5] Central to the development of this technology is the nanofabrication of arrays of DNA and proteins. Such arrays have influenced the areas of genomics and proteomics because of their ability to simultaneously detect a large number of molecular species or 'multiplex'. The miniaturization of bioassays has been eagerly pursued in an effort to achieve enhanced performance such as shorter response times, smaller sample volumes, and higher sensitivities.[6–9] Dip-pen nanolithography (DPN) was developed to write nanoscale patterns directly on substrates.[10,11] Among the many applications of this technology is the ability to pattern modified oligonucleotides on gold and silicon oxide surfaces. Here, feature sizes can range from a few micrometers to less than 50 nm.[12] In a typical DNA-patterning experiment with DPN, the surfaces of silicon nitride atomic force microscopy (AFM) cantilevers are chemically modified for increased tip hydrophilicity. This step is used to improve the coating efficiency of the DNA molecules. A more attractive way of delivering inks in DPN mode is through the use of microfluidics that can deliver different inks to specific tips within a cantilever array. This approach, when it has been successfully developed, will provide greater flexibility and increased utility of DPN for the generation of combinatorial bioarrays.

Other recent approaches to biomolecular patterning include the use of microfluidic components such as reservoirs, microchannels, and small apertures or slots to control the delivery of chemical solutions.[13–21] Such tools do not require tip coating because samples are directly delivered onto a surface in a solution. However, the reported resolution of microfluidic tools is about 1 μm at best because of limitations from the geometries of the apertures or slots that control the molecular writing mechanisms in these devices.

Herein, we present the patterning of DNA molecules on the submicrometer length scale using a volcano-like tip. This eliminates the need for tip-surface modification by implementing direct delivery of a solution containing DNA molecules to the tip. As a microfluidic AFM probe, the nanofountain probe (NFP) was reported to allow high-resolution writing and have advantages for delivery of molecular inks in solution.[22–23] A feature size as small as 40 nm was demonstrated with thiol molecules. The NFP was microfabricated to integrate an on-chip reservoir, microchannels, and a volcano-like dispensing tip.

Following the development of the first generation NFP, a single-probe system,[22–23] we made augmentations to produce a linear array of 12 NFP cantilevers with two on-chip reservoirs on each side of the chip, Figure 1.[24] The cantilever lengths on each side were 630 and 520 μm, respectively. Each reservoir fed six adjacent cantilevers to achieve simultaneous patterning with two molecular species. The NFP chip was designed to fit commercially available AFM instruments and utilized the instrument scanner, optical detection, and feedback control to engage surfaces. While one cantilever was selected for the feedback control of the chip, the other cantilevers made passive contact with the surface by adjustment of the tilting angle between the array and the substrate. The multiple-tip, double-ink patterning with this linear-array NFP chip was recently demonstrated.[24] More recently, a third generation of the NFP was fabricated. Modifications for this NFP included the possibility of fabrication on silicon-on-insulator (SOI) wafers, improved channel sealing, deeper channels to allow the delivery of larger particles, and more robust fabrication processes that led to enhanced yield and better control of

[*] Prof. H. D. Espinosa, Dr. K.-H. Kim, A. M. Ho, Prof. N. Moldovan
Department of Mechanical Engineering, Northwestern University
2145 Sheridan Road, Evanston, IL 60208 (USA)
E-mail: espinosa@northwestern.edu
Dr. R. G. Sanedrin, Prof. C. A. Mirkin
Department of Chemistry, Northwestern University
2145 Sheridan Road, Evanston, IL 60208 (USA)
Dr. S. W. Lee
School of Chemical Engineering and Technology
Yeungnam University, Kyongsan 712-749 (Korea)

[**] This work was supported primarily by the Nanoscale Science and Engineering Initiative of the National Science Foundation under NSF Award Number EEC–0118025. HDE acknowledges the support provided by the National Science Foundation through NIRT project No. CMS00304472. CAM acknowledges the AFOSR, ARO, and DARPA for generous support. CAM is also grateful for a NIH Director's Pioneer Award. The authors acknowledge the Microfabrication Applications Laboratory (MAL) of the University of Illinois at Chicago, the Cornell NanoScale Science & Technology Facility (CNF) of Cornell University, the Materials Processing and Crystal Growth Facility (MPCGF) of Northwestern University, Northwestern University Atomic- and Nanoscale Characterization Experimental Center (NUANCE), and the Electron Microscopy Center (EMC) of Argonne National Laboratory for the fabrication and characterization facilities.

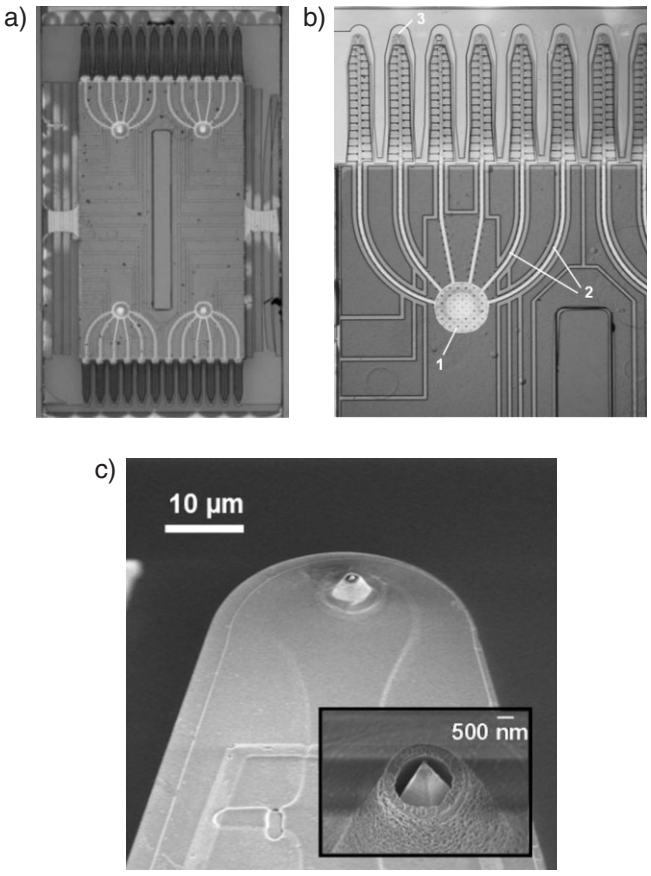

Figure 1. Second generation NFP chip. a) Optical image of the front-side view of an NFP chip. b) Close-up optical image of the chip: 1) on-chip reservoir, 2) microchannels, and 3) the volcano tip. c) SEM image of a cantilever integrated with a volcano tip at the end; in the inset a close-up of the volcano tip is shown.

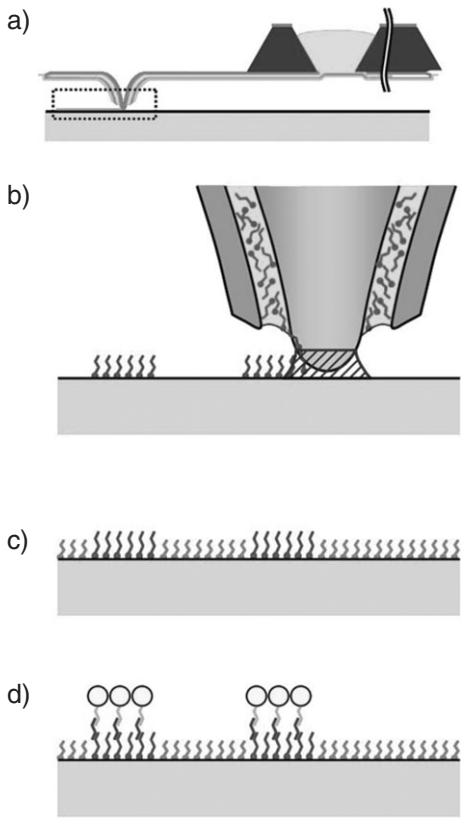

Figure 2. Schematic of experimental procedure, a) molecular-ink feeding, b) direct patterning of alkanethiol-modified oligonucleotides on a Au substrate, c) passivation of the unpatterned areas with C6 thiol to avoid unspecific binding, d) hybridization of the linker and probe DNA strands.

the tip geometry. The linear arrays of 12 cantilevers were also shortened on each side of the chip, to 520 and 430 μm, respectively. Both the second and third generation NFPs demonstrated their ability to pattern single-stranded oligonucleotides without tip modification. This is the focus of this article.

As shown in Figure 2, we employed the NFP to pattern a gold surface with alkanethiol-modified oligonucleotides. The patterned DNA spots were subsequently hybridized with complementary DNA-functionalized Au nanoparticles (~15 nm in diameter) to probe bioactivity. The system of choice to demonstrate the writing capabilities of the NFP chips and subsequent bioactivity of the deposited strands was a three-strand DNA system containing a thiolated DNA strand (capture DNA), a DNA strand conjugated to 15-nm-diameter gold nanoparticles (probe DNA), and a linker DNA strand (linker DNA) that links the capture and the probe DNA.

Upon contact between the nanofountain probe and the substrate, dot patterns of capture DNA were generated using various contact times. An array of capture oligonucleotides (20 × 20 μm) consisting of dot features of (180±25), (300±34), and (422±25) nm were generated with the second generation NFP by holding times of 0.5, 1.0, and 2.0 s, respectively. The effect of contact time on feature size is clearly seen in Figure 3. It is interesting to note that the same tips could be used repeatedly through days of experiments with several extra feedings.

In the dark-field optical micrograph, the assembled nanoparticles were identified by the scattered light, Figure 3a. The image clearly shows spot sizes that correlate with the contact time. Rows 1 and 4 correspond to 2 s of contact time while rows 2 and 5 were obtained with a contact time of 1 s. Rows 3 and 6, corresponding to a contact time of 0.5 s, are almost imperceptible in this image because the spot size falls below the resolution limit of the dark-field optical microscopy technique. The AFM topography image (Fig. 3b) was obtained in tapping mode and the measured height of the features was ~20 nm (Fig. 3c). Scanning electron microscopy (SEM) was also used to image the patterned spot arrays (Fig. 3d). The spot size and shape revealed by the SEM image agrees very well with the AFM topographic information. Furthermore, the magnified SEM image, Figure 3e, confirms the hybridization of the DNA functionalized gold nanoparticles to the NFP-generated capture DNA template. The smallest spot size corresponds to a contact time of 0.5 s. The routine minimum spot size, identified from several experiments using the NFP, was 200–300 nm in diameter.

ADVANCED MATERIALS

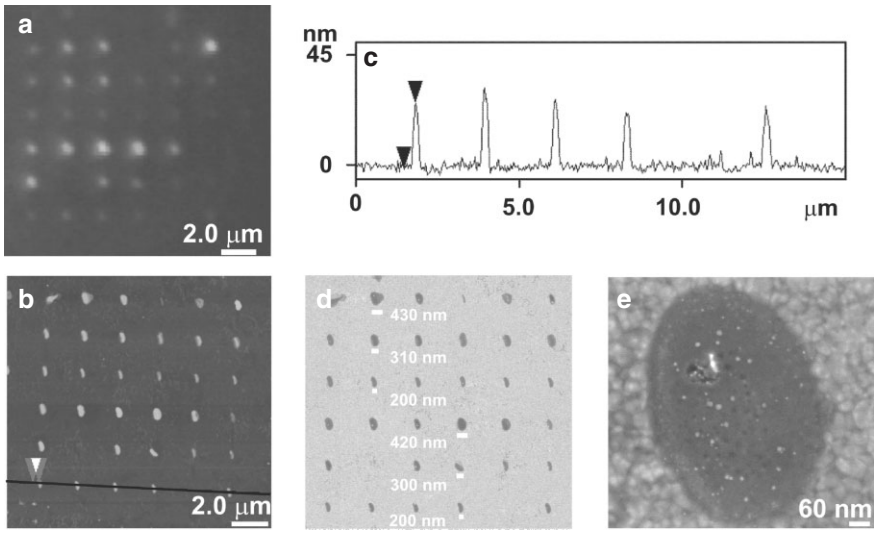

Figure 3. Array of dots patterned with three different contact times of 2, 1, and 0.5 s, for each alternating row of the array, a) dark-field optical image of the dot array after hybridization. Light scattered by the Au particles attached on the array was used. b) AFM topography image and c) height profile of the same array, acquired in tapping-mode operation. d) and e) SEM image of dot array and single dot, respectively. Multiple Au nanoparticles are visible in (e).

The third generation NFP was employed to obtain highly reproducible pattern geometries, as indicated in Figure 4. Dot patterns with contact times of 10, 5 and 2 s were successfully fabricated over a relative humidity range of 20–90 % at room temperature. Small differences in feature size are observed as a function of humidity and contact time. Repeatedly halving the amount of dimethylformamide (DMF) in the DNA solution to increase its evaporation rate, and increasing the tilt of the NFP against the substrate to reduce the contact area of the fountain-probe tip resulted in very round dots, as shown in Figure 5.

The biological activity that was obtained demonstrated the submicrometer patterning capability of the NFP with DNA strands directly delivered through microfluidic channels. Moreover, the NFP is superior to other aforementioned microfluidic devices in terms of the minimum attainable feature size. For example, in the case of DPN with nanopipettes, the spot sizes tend to be larger than the contact area of the pipette tip with the substrate.[13,14] The feature size is usually above 1 μm and the fabrication method by pulling individual capillary tubes does not lead to reproducible tip orifices that are needed for the resolutions reported herein. Furthermore, the fabrication method is not suitable for scaling to high-throughput two-dimensional (2D) arrays. In another approach, apertures were created at the apex of pyramidal tips using either microfabrication techniques or focused ion beam (FIB) milling.[16,17] The hollow back of the apertured pyramidal tip was used as a reservoir. Deposition of the liquid was achieved by contacting the tip with a substrate. The resulting spot sizes were well above 1 μm.

In the case of cantilevers or tips with a slot at the end, the resolution is determined by the size of the gaps between the split. For example, stainless steel pens were microfabricated to have a slot gap of 30 μm and the generated spot sizes were 10–30 μm wide and 20–140 μm long.[18] In another report, microcantilever spotters were used to generate spot sizes greater than 10 μm in diameter.[20] The surface patterning tool (SPT), a miniaturized cantilever-based tool that is another variant of DPN, was also reported. With this tool, 1-μm-split gap patterned spot sizes of 2–3 μm.[21] Since the slot gaps of such tools are created by conventional photolithographic processes, it is challenging to reduce the size of the gaps to less than 1 μm unless alternative high-resolution lithography techniques are employed such as electron beam lithography or projection lithography with a phase-shift mask.

While the NFP also delivers a sample solution through an enclosed channel, its superior performance is a result of its

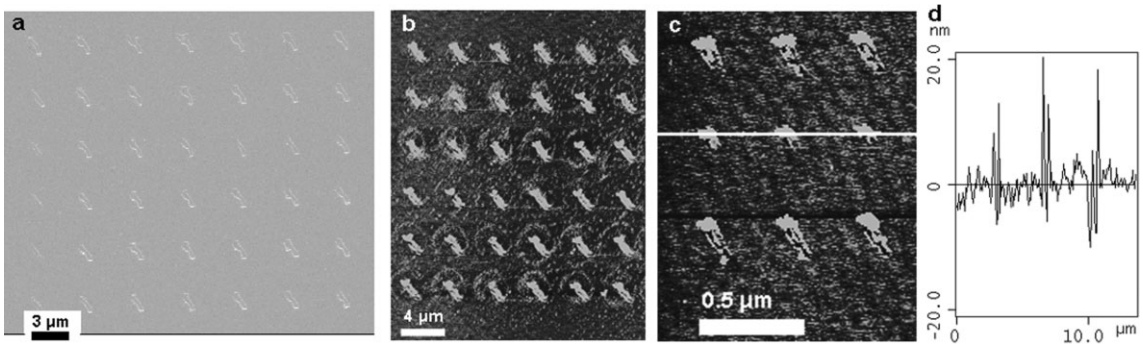

Figure 4. a) SEM and b) AFM images of a dot array patterned by the third generation NFP c) AFM topography image and d) height profile along the line in (c), acquired in tapping mode operation.

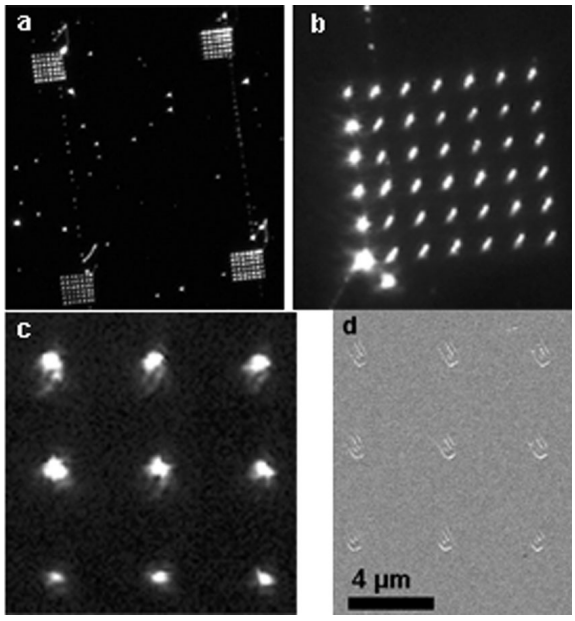

Figure 5. Optical images of a) Multiple-dot arrays patterned by two adjacent cantilevers of the third generation NFP after hybridization. b) Enlargement of array at bottom left of (a). c) Dots patterned with different contact times in each row of 10, 5, and 2 s. d) SEM image of dot array.

volcano-like dispensing tip. Under the appropriate wetting conditions, which can be controlled through buffer chemistry, the solution delivered through the microchannel stops at the ring-shaped aperture of the volcano tip to form an air-liquid interface, Figure 2b.[25] Subsequently, the molecules move out of the interface to diffuse along the surface of the inner tip and then to the substrate. In this sense, the final deposition mechanism is the same as that of conventional DPN. This is somewhat different from nanopipette tools in which the solution directly touches the surface for the deposition of the molecules. This occurs when the tip is brought into contact with a surface. Additionally, the integrated microchannel of the NFP is enclosed while that of the SPT is open. Open-type channels are simple to fabricate, relatively clog-free, and easier to clean. However, such open microfluidic elements are prone to cross contamination when different types of inks are used, such as in multiple-tip and multiple-ink patterning. Also, evaporation may play a critical role in certain applications because enclosed microchannels can reduce the evaporation rate of the molecular solution.

In addition to superior patterning resolution, the NFPs are scalable for use in arrays because they are fabricated by standard microfabrication techniques. It is known that high-throughput capability is indispensable for the realization of rapid manufacture of bioassays. In this context, it is worth mentioning that parallel operation of scanning probes has been pursued in an effort to improve the low throughput of single-tip scanning systems.[26–28] In the DPN technique, the throughput limitation was improved using custom-made linear arrays of up to 250 tips [29a] and more recently through the development of 2D 55000-pen arrays.[29b] These arrays demonstrated parallel writing of alkanethiol inks over the centimeter length scale with impressive throughput for generating nanostructures at a rate of ~7.0×10^6 dots min^{-1} (assuming 100-nm-diameter dots). Parallelization of the SPT DPN approach was also reported with a one-dimensional (1D) array of 5 cantilevers integrated with 5 corresponding reservoirs to demonstrate patterning of multisample-biomolecular arrays.[30] The scalability of the SPT arrays is limited to 1D arrays because their cantilevers are not integrated with AFM-type tips and thus their operation requires tilting of the array against the target substrate. In contrast, the NFP can be expanded to 2D arrays with a network of reservoirs and microchannels because the NFP cantilevers have protruding tips that eliminate the need for tilting cantilevers against the substrate surface. Furthermore, the feasibility of integrating piezoelectric-bending actuators onto the NFP array has been demonstrated by our group.[32] With active probes, with the ability to lift tips off substrates, independent patterns can be made simultaneously on individual writing sites. Lastly, the patterning of other biomolecules such as proteins using the NFP is currently being explored.

In summary, the *direct delivery* of biomolecules was achieved by NFP technology without the need for tip modification. The capability that has been demonstrated is expected to impact the nanofabrication of bioassays, especially when tips are to be arranged as 1D or 2D arrays for wafer-level processes with multiple molecular inks. The NFP volcano-tip also proved to be capable of high-resolution writing of biomolecules in the submicrometer domain. Furthermore, the results and scalability of the NFP to 2D arrays described here suggest that there are possibilities for building nanoscale bioassays, at the wafer level, using a large variety of biomolecules including proteins and viruses.

Experimental

In a typical experiment, a solution containing 6.60 μL of 0.1 M phosphate buffer (PBS) (pH 7.4), 3.06 μL of DMF, and 0.34 μL of solution containing 0.3 M $MgCl_2$ and 10 mM capture DNA (3′ HS-$(CH_2)_3$-A10-TAG GAA ATG TTA TAA 5′) was fed into the on-chip reservoir using a micropipette. The chip was immediately mounted on an AFM instrument (Thermomicroscopes CP) that was housed in a humidity controlled glovebox. All experiments using the second generation NFPs were carried out at a relative humidity of (70±5) %, at room temperature. Experiments using third generation NFPs were performed at a relative humidity in the range of 20–90 %.

After DNA patterning, the unpatterned areas of the Au substrate were passivated by immersing the substrate in a solution of 1.0 mM hexanethiol (HT) for 10 min. The substrates were then rinsed with copious amounts of ethanol and water, and dried with nitrogen. For hybridization experiments, 60 μL of a 10 nM probe DNA solution (Au nanoparticle–S-$(CH_2)_6$O-A10-GAG GGA TTA TTG TTA 3′) was first hybridized with the linker DNA strands (5′ ATC CTT TAC AAT ATT TAA CAA TAA TCC CTC 3′). The NFP-generated capture DNA dot features and the DNA duplex (linker and probe DNA) were then hybridized by immersing the substrates in the DNA duplex solution for 40 min at 37 °C. The substrates were then rinsed with ammonium acetate buffer. The hybridization of the Au nanoparticles to

ADVANCED MATERIALS

the spots within the array was verified by dark-field optical microscopy and tapping mode AFM topography (Fig. 3).

Received: May 23, 2007
Revised: October 8, 2007
Published online: December 20, 2007

[1] K.-B. Lee, J.-H. Lim, C. A. Mirkin, *J. Am. Chem. Soc.* **2003**, *125*, 5588.
[2] J.-H. Lim, D. S. Ginger, K.-B. Lee, J. Hoe, J.-M. Nam, C. A. Mirkin, *Angew. Chem., Int. Ed.* **2003**, *42*, 2309.
[3] J.-M. Nam, S. W. Han, K.-B. Lee, X. Liu, M. A. Ratner, C. A. Mirkin, *Angew. Chem., Int. Ed.* **2004**, *43*, 1246.
[4] R. A. Vega, D. Maspoch, K. Salaita, C. A. Mirkin, *Angew. chem., Int. Ed.* **2005**, *44*, 6013.
[5] D. L. Wilson, R. Martin, S. Hong, M. Cronin-Golomb, C. A. Mirkin, D. L. Kaplan, *Proc. Natl. Acad. Sci. USA* **2001**, *93*, 13660.
[6] M. Schena, D. Shalon, R. W. Davis, P. O. Brown, *Science* **1995**, *270*, 467.
[7] R. J. Lipshutz, S. P. A. Fodor, T. R. Gingeras, D. J. Lockhart, *Nat. Genet.* **1999**, *21*, 20.
[8] G. MacBeath, S. L. Schreiber, *Science* **2000**, *289*, 1760.
[9] M. J. Heller, *Annu. Rev. Biomed. Eng.* **2002**, *4*, 129.
[10] R. D. Piner, J. Zhu, F. Xu, S. Hong, C. A. Mirkin, *Science* **1999**, *283*, 661.
[11] a) D. S. Ginger, H. Zhang, C. A. Mirkin, *Angew. Chem., Int. Ed.* **2004**, *43*, 30. b) D. A. Weinberger, S. G. Hong, C. A. Mirkin, B. W. Wessel, T. B. Higgins, *Adv. Mat.* **2000**, *12*, 1600. c) H. Zhang, S. W. Chung, C. A. Mirkin, *Nano Lett.* **2003**, *3*, 43.
[12] L. M. Demers, D. S. Ginger, S.-J. Park, Z. Li, S.-W. Chung, C. A. Mirkin, *Science* **2002**, *296*, 1836.
[13] A. Lewis, Y. Kheifetz, E. Shambrodt, A. Radko, E. Khatchatryan, C. Sukenik, *Appl. Phys. Lett.* **1999**, *75*, 2689.
[14] H. Taha, R. S. Marks, L. A. Gheber, I. Rousso, J. Newman, C. Sukenik, A. Lewis, *Appl. Phys. Lett.* **2003**, *83*, 1041.
[15] A. Bruckbauer, L. M. Ying, A. M. Rothery, D. J. Zhou, A. I. Shevchuk, C. Abell, Y. E. Korchev, D. J. Klenerman, *J. Am. Chem. Soc.* **2002**, *124*, 8810.
[16] A. Meister, S. Jeney, M. Liley, T. Akiyama, U. Staufer, N. F. de Rooij, H. Heinzelmann, *Microelectron. Eng.* **2003**, *67–68*, 644.
[17] A. Meister, M. Liley, J. Brugger, R. Pugin, H. Heinzelmann, *Appl. Phys. Lett.* **2004**, *85*, 6260.
[18] M. O. Reese, R. M. van Dam, A. Scherer, S. R. Quake, *Genome Res.* **2003**, *13*, 2348.
[19] P. Belaubre, M. Guirardel, G. Garcia, J. B. Pourciel, V. Leberre, A. Dagkessamanskaia, E. Trevisiol, J. M. Francois, C. Bergaud, *Appl. Phys. Lett.* **2003**, *82*, 3122.
[20] P. Belaubre, M. Guirardel, V. Leberre, J. B. Pourciel, C. Bergaud, *Sens. Actuators, A.* **2004**, *110*, 130.
[21] J. Xu, M. Lynch, J. L. Huff, C. Mosher, S. Vengasandra, G. Ding, E. Henderson, *Biomed. Microdevices* **2004**, *6*, 117.
[22] K.-H. Kim, N. Moldovan, H. D. Espinosa, *Small* **2005**, *1*, 632.
[23] N. Moldovan, K.-H. Kim, H. D. Espinosa, *J. Microelectromech. S.* **2006**, *15*, 204.
[24] N. Moldovan, K.-H. Kim, H. D. Espinosa, *J. Micromech. Microeng.* **2006**, *16*, 1935.
[25] K.-H. Kim, C. Ke, N. Moldovan, H. D. Espinosa, *Mater. Res. Soc. Symp. Proc.* **2003**, *782*, A5.56.1.
[26] M. Zhang, D. Bullen, S.-W. Chung, S. Hong, K. S. Ryu, Z. Fan, C. A. Mirkin, C. Liu, *Nanotechnology* **2002**, *13*, 212.
[27] P. Vettiger, M. Despont, U. Drechsler, U. Durig, W. Haberle, M. I. Lutwyche, H. E. Rothuizen, R. Stutz, R. Widmer, G. K. Binnig, *IBM J. Res. Dev.* **2000**, *44*, 323.
[28] S. C. Minne, J. D. Adams, G. Yaralioglu, S. R. Manalis, A. Atalar, C. F. Quate, *Appl. Phys. Lett.* **1998**, *73*, 1742.
[29] K. Salaita, S. W. Lee, X. Wang, L. Huang, T. M. Dellinger, C. Liu, C. A. Mirkin, *Small* **2005**, *1*, 940.
[30] J. Xu, M. Lynch, S. Nettikadan, C. Mosher, S. Vegasandra, E. Henderson, *Sens. Actuators, B* **2006**, *113*, 1034.
[31] S. Hong, C. A. Mirkin, *Science* **2000**, *288*, 1808.
[32] http://clifton.mech.northwestern.edu/~nfp/

